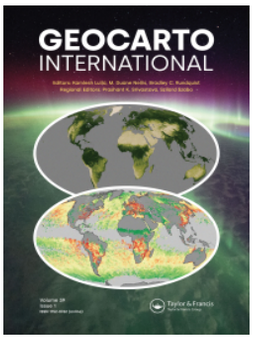

Geocarto International

ISSN: (Print) (Online) Journal homepage: www.tandfonline.com/journals/tgei20

Unveiling the mineral resources and structural patterns in the Middle Benue Trough: a comprehensive exploration using airborne magnetic and radiometric data

Stephen E. Ekwok, Anthony M. George, Asuquo A. Omori, Kamal Abdelrahman, Samuel I. Ugar, Peter Andráš, Morod I. Morphy, Anthony E. Akpan & Ahmed M. Eldosouky

To cite this article: Stephen E. Ekwok, Anthony M. George, Asuquo A. Omori, Kamal Abdelrahman, Samuel I. Ugar, Peter Andráš, Morod I. Morphy, Anthony E. Akpan & Ahmed M. Eldosouky (2024) Unveiling the mineral resources and structural patterns in the Middle Benue Trough: a comprehensive exploration using airborne magnetic and radiometric data, Geocarto International, 39:1, 2339290, DOI: 10.1080/10106049.2024.2339290

To link to this article: https://doi.org/10.1080/10106049.2024.2339290

Published online: 16 Apr 2024.

GEOCARTO INTERNATIONAL
2024, VOL. 39, NO. 1, 2339290
https://doi.org/10.1080/10106049.2024.2339290

Unveiling the mineral resources and structural patterns in the Middle Benue Trough: a comprehensive exploration using airborne magnetic and radiometric data

Stephen E. Ekwok[a], Anthony M. George[a], Asuquo A. Omori[a], Kamal Abdelrahman[b], Samuel I. Ugar[c], Peter Andráš[d], Morod I. Morphy[c], Anthony E. Akpan[a] and Ahmed M. Eldosouky[e]

[a]Applied Geophysics Programme, Department of Physics, University of Calabar, Calabar, Nigeria; [b]Department of Geology & Geophysics, College of Science, King Saud University, Riyadh, Saudi Arabia; [c]Department of Geology, University of Calabar, Calabar, Nigeria; [d]Faculty of Natural Sciences, Matej Bel University, Banska Bystrica, Slovakia; [e]Department of Geology, Faculty of Science, Suez University, Suez, Egypt

ABSTRACT

The Middle Benue Trough (MBT) in Northcentral Nigeria is a geologically significant area with vast mineral resource potential. Employing airborne magnetic and radiometric data, this study utilized the Centre for Exploration Targeting on enhanced total magnetic intensity data to reveal geologic structures, lithological units and mineralization zones. Lineaments predominantly trended in NE-SW direction, with noteworthy orientations in NNE-SSW and E-W. Radiometric anomalies correlated with distinct lithological units, pinpointing granitic gneiss, alluvium, shale, siltstone and sandstone. A magnetically concentrated and potassium-rich area indicated potential polymetallic-magnetic mineralization. The 2D model illustrated igneous intrusions influencing prevalent geologic structures, such as sediment baking and doming. Thorough analysis, including source parameter imaging, standard Euler deconvolution and 2D forward modelling, revealed sediment thicknesses below 1500 m. This research enhances understanding of the MBT's geological features, offering valuable insights for mineral exploration and resource assessment in the region.

ARTICLE HISTORY
Received 18 January 2024
Accepted 1 April 2024

KEYWORDS
Magnetic data; radiometric data; geologic structures; centre for exploration targeting; Middle Benue Trough

Introduction

The development of the Nigerian Benue Trough and Basement Complexes were viewed in the light of global tectonic and tectonothermal events respectively (Burk and Dewey 1974). Over time, geologic structures in the Precambrian regions were triggered by the younger granites (Woakes et al. 1987). Likewise, the Cretaceous Benue Trough was massively invaded by the Santonian-Recent basic and intermediate igneous intrusions

CONTACT Ahmed M. Eldosouky ahmed.eldosouky@sci.suezuni.edu.eg

(Benkhelil 1987; Ekwok et al. 2019). These tectonic events caused to the creation of different geologic structures, chemical processes and hydrothermal alterations of the host rocks. Several researchers have investigated the metallogeny of the Nigerian basement (Orajaka 1973; Olade 1980; Woakes et al. 1987; Haruna 2017), the occurrence of coal, limestones, ironstones (Oladapo and Adeoye-Oladapo 2011; Ene et al. 2012) and the coexistence of brine fields alongside barite veins and lead-zinc (Uma 1998) in the Benue Trough. The mineral belts are linked to deeply buried geologic structures possibly extending down to the upper mantle (Haruna 2017). The geologic structures serve as pathway for hydrothermal fluid (rich in gold, copper, lead and zinc) movement and deposition (Dill et al. 2010, 2013; Mineral Resources of the Western US 2017). The application of potential field methods and improved edge detection procedures in an integrated programs have been effective in the delineation of buried geologic structures and location of new zones of mineralisation (Woakes et al. 1987).

The Middle Benue Trough, situated in Northcentral Nigeria, represents a region of huge geological significance with the potential for diverse mineral resources (Adekeye and Yakubu 2016). The Middle Benue Trough (MBT) which is a segment of the larger Benue Trough, is a major sedimentary basin resulting from the separation of the West African and Congo Cratons during the Mesozoic era (Reyment 1965; Ugwu et al. 2015; Osuji et al. 2018). The rift basin has a complex tectonic history, making it a favourable environment for the formation of various rift mineral deposits, including metallic ores and industrial minerals (Obaje 2009; Carruth 2011; Akpan et al. 2014; Adeyemo et al. 2018). Mineral explorations in the MBT involving ground geophysical surveys, geological field mapping, geochemical sampling and drilling, have been stalled by numerous challenges, like high costs, low spatial coverage due to remote and rugged terrains, thick sedimentary cover, complex structural framework and the lack of comprehensive geological information (Obaje 2009; McClenaghan 2017; Adeyemo et al. 2018; Mihalasky et al. 2018). Presently, airborne geophysical surveys have gained prominence as effective tools for mineral exploration due to their ability to rapidly cover large areas and provide valuable information about subsurface geology (Dentith and Mudge 2014; McClenaghan 2017; Mihalasky et al. 2018; Araujo et al. 2019).

The Nigerian Geological Survey Agency has been in charge of large-scale acquisition of airborne geophysical data and geological mapping. These data provide a valuable base for further detailed geoscience investigations. Delineation of prominent and subtler geologic structures is possible because of the availability of improved filters as well as high speed and robust computer program (Elkhateeb and Eldosouky 2016; Oha et al. 2016). Airborne geophysical techniques (mostly magnetic and radiometric surveys) have emerged as valued tools for regional-scale mineral assessment (Nabighian 1972; Dentith and Mudge 2014; McClenaghan 2017; Ebbing et al. 2019; Reid et al. 2019). The blend of magnetic and radiometric methods offers significant advantages in mineral exploration (Adekeye and Yakubu 2016; Ayodele et al. 2018; Blinman et al. 2018; Marshall 2021). These methods permit multidimensional interpretation, providing vital information about lithological disparities, structural controls and probable mineralization targets in different geological settings (Dare et al. 2017; McClenaghan 2017; Blinman et al. 2018; Arora et al. 2019; Marshall 2021). On the whole, the exploration of mineral resources in the MBT has been significantly advanced by the application of potential field and radiometric surveys. For instance, aeromagnetic data have been used to identify potential areas rich in ferrous minerals, map heavy mineral concentrations (like copper, lead and zinc) and assess the uranium potential (Kasidi and Ndatuwong 2017; Anudu et al. 2020; Emeka and Usman 2020; Salawu et al. 2020).

Magnetic and radiometric techniques have been carried out by geoscientists to define hydrothermal alteration zones and regions characterized by magnetic and gamma-ray signatures (Ekwok, Akpan, and Kudamnya 2020). The investigation of anomalies that are associated with polymetallic and Copper-Uranium mineralization have been done (eg Geological Survey of Canada 1992; Shives et al. 1995; Boadi et al. 2013). However, polymetallic minerals were observed in zones with the highest coincident of potassium and magnetic strength (Boadi et al. 2013; Dill et al. 2013; Ekwok, Akpan, and Kudamnya 2020). Studies by Shives et al. (1995) involving magnetic, radiometric and VLF-EM techniques to investigate polymetallic-magmatic hydrothermal deposits at Lou Lake revealed the occurrence of lead, zinc, copper, silver and gold. Additionally, a variety of volcanically associated gold, massive sulphide and base metals are often connected to potassium alterations in the form of sericite (Shives et al. 1997). Alterations related to potassium feldspar in volcanic zones are usually associated with massive sulphide, base metal, gold and several other kinds of deposits that are shear-hosted (Offler and Whitford 1992).

The aeromagnetic method is a useful tool for detecting anomalous geological structures, as well as mapping the regional geology of the basement (Beckett 2003; Ekwok et al. 2019; Ekwok, Akpan, Ebong, and Ece 2021; Ekwok, Akpan and Ebong 2021). Furthermore, the magnetic method is often employed in mineral explorations (Ekwok, Akpan, and Kudamnya 2020), the outlining of regional surficial geologic boundaries and mapping of geologic structures (Ekwok et al. 2019; Ekwok, Akpan, Kudamnya, and Ebong 2020; Ekwok, Akpan, Achadu, et al. 2021; Ekwok, Akpan and Ebong 2021; Ekwok, Achadu, et al., 2022; Ekwok, Akpan, Achadu, and Ulem, 2022; Ekwok, Eldosouky, Achadu, et al. 2022). It can be engaged in archaeological studies, geothermal exploration (Ben et al. 2022, 2023; Abdelrahman et al. 2023; Alfaifi et al. 2023), reconnaissance hydrocarbon investigations (Telford et al. 1990), detection of unexploded ordnance (UXO), (Essa and Elhussein 2018) among others. Over time, there has been a tremendous upgrading in the many procedures for filtering, modelling and interpretation of magnetic data. Yet, the solution is unstable and non-unique because of the inverse problem that is often related to magnetic data (Essa and Elhussein 2017). However, having sufficient geological knowledge and applying the right advanced techniques for data reduction, enhancement, modelling and interpretation, dependable can generate a dependable solution (Essa and Elhussein 2018).

Gamma-ray surveys, which have previously helped identify uranium, thorium and potassium (Shives et al. 1997), can be used in multi-element studies (Ekwok, Eldosouky, Ben, et al. 2022; Eldosouky et al. 2022, 2023; Ekwok et al. 2023). Additionally, the method can be used to investigate natural and man-made radionuclides and enhance geological characterizations, especially in regions with complex geology (Lee et al. 2001; Abdelrahman et al. 2006). Likewise, it can be useful in environmental monitoring programs (Shives et al. 1997; Lee et al. 2001; Paoletti and Pinto 2004). Nevertheless, a thorough knowledge of geochemistry, petrology, bedrock and surficial geology, plus complementary geophysical technique(s), is required for the proper interpretation of gamma-ray spectrometric anomalies (Shives et al. 1997).

In this research, airborne magnetic and radiometric data collected over the MBT were employed. This study provides an extensive analysis of the application of Centre for Exploration Targeting (CET) on enhanced magnetic data involving filters like ASIG, FVD, TAD and THD. As well, image analysis was applied to the radiometric data while the SPI, SED and 2D modelling were applied to the magnetic data. These procedures have aided the delineation of geologic structures, mapping of areas with coextensive high

magnetization and potassium concentration, generation of important information on the lithology and locations of radioactive minerals.

Location and geology of Middle Benue Trough

The MBT, a subset of the larger Benue Trough, is a key geological basin located in the central part of Nigeria. The study area (Figure 1) has a complex geological history characterized by tectonic events, sedimentary deposition and structural development (Reyment 1965).

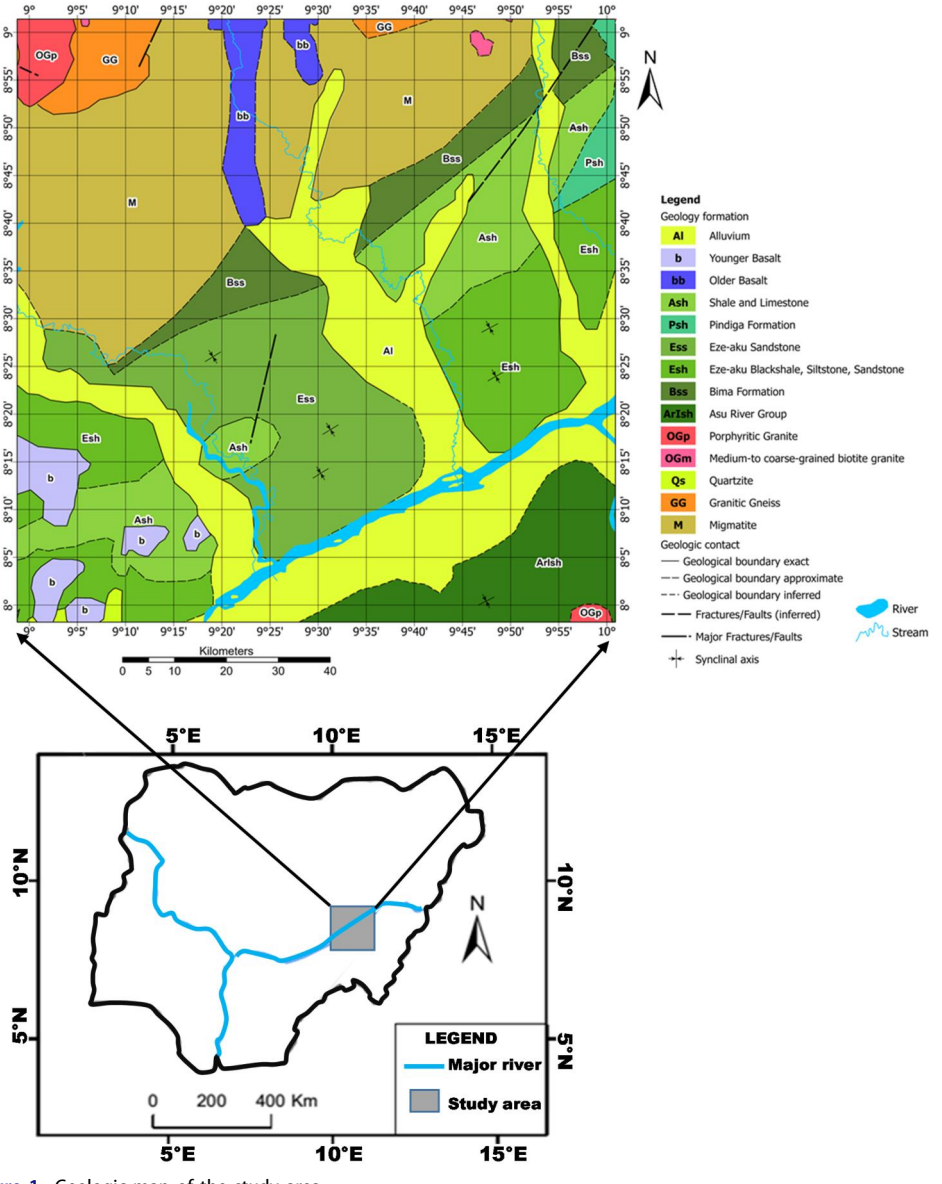

Figure 1. Geologic map of the study area.

The tectonic history of the MBT is basically connected to the rifting of the African Plate in the Cretaceous period (Ajayi 1976). This rift phase led to the creation of a graben-like structure, which later evolved into a passive margin in the Cretaceous, marked by sedimentary buildup in lacustrine, fluvial and deltaic environments (Obaje 2009). Subsequent tectonic phases involved compression in the Neogene, resulting in numerous faults, folds and unconformities in the MBT (Ajayi et al. 2008). These structures have a significant influence on the distribution of mineral resources within the trough, including limestone, gypsum and lead-zinc deposits (Okunlola et al. 2015).

Stratigraphically, the MBT comprises an assorted series of sedimentary rocks like shale, sandstone, limestone and conglomerates, which represent diverse geological epochs and environmental settings (Reyment 1965). The lowermost units comprise basement rocks, primarily composed of Precambrian gneisses, schists and granite (Reyment 1965). Overlying these are sedimentary sequences of the Cretaceous and Neogene periods, exhibiting disparities in lithology and fossil content (Ajakaiye 1976).

Data acquisition and method

The reduced magnetic and radiometric datasets used in this study were acquired by Fugro Airborne Services, Canada, from 2005 to 2010. These data were measured using the Flux-Adjusting Surface Data Assimilation System with tie line space of 500 m, flight-line space of 100 m and terrain clearance ranging from 80 to 100 m.

Aero-radiometric studies are founded on the measurement of gamma rays caused by the decay of natural potassium (K), thorium (Th) and uranium (U) in near-surface soil/rock (Ranjbar et al. 2001). An assimilated system with components of an Advanced Digital Spectrometer (ADS model RS-500) for every crystal in the detector box was fixed on a Cessna Caravan fixed-wing aircraft. The ADS which is a high-resolution (1024 channel) gamma spectrometer, was used for measurement at mean terrain clearance of 80 m. Studies by Wemegah et al. (2015) and others have shown that gamma-rays are immensely reduced with depth as most of the radiations emanate from near the surface of the Earth, with about 90% of the acquired gamma-rays originating from the overburden materials (30–45 cm) with a density of 1.5 g/cm^3. Also, relative radiometric correction was applied to diminish atmospheric and other unanticipated disparities amongst numerous images by altering the radiometric properties of target imageries to suit the base image. The magnetic and radiometric datasets used in the study were obtained from the Nigerian Geological Survey Agency.

In this study, enhancement operations enhancement techniques like the ASIG, FVD, TAD and THD, were applied to the total magnetic intensity data (Figure 2). The magnetic data was filtered by applying procedures that heighten the structures emanating from geologic bodies (Milligan and Gunn 1997). The enhanced magnetic maps (Figure 3) were further filtered using CET in order to generate structural maps.

Maximum responses directly over magnetic anomalies are produced using the ASIG (Nabighian 1972, 1984). This method is widely used at low magnetic latitudes due to the typical difficulty involved with the reduction-to-pole procedure. Roest et al. (1992) applied three orthogonal derivatives of the magnetic data to describe the amplitude of the ASIG:

$$\left|ASIG_{(x,y)}\right| = \sqrt{\left(\frac{\partial A}{\partial x}\right)^2 + \left(\frac{\partial A}{\partial y}\right)^2 + \left(\frac{\partial A}{\partial z}\right)^2} \tag{1}$$

the measured magnetic data defined by A in Equation (1).

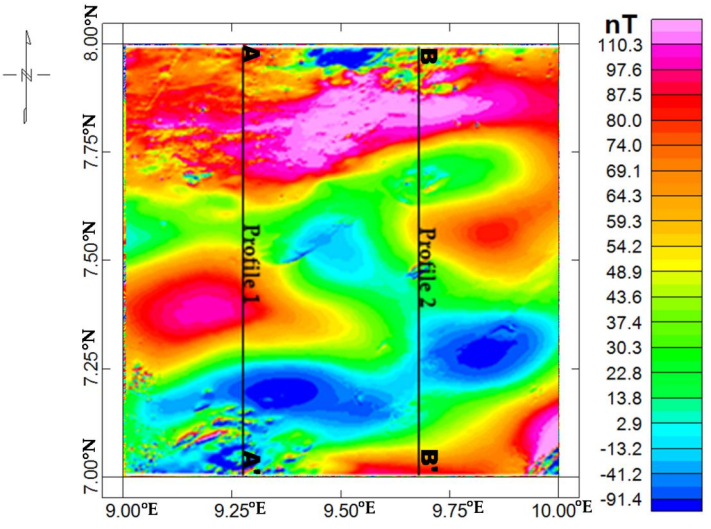

Figure 2. Total magnetic intensity map.

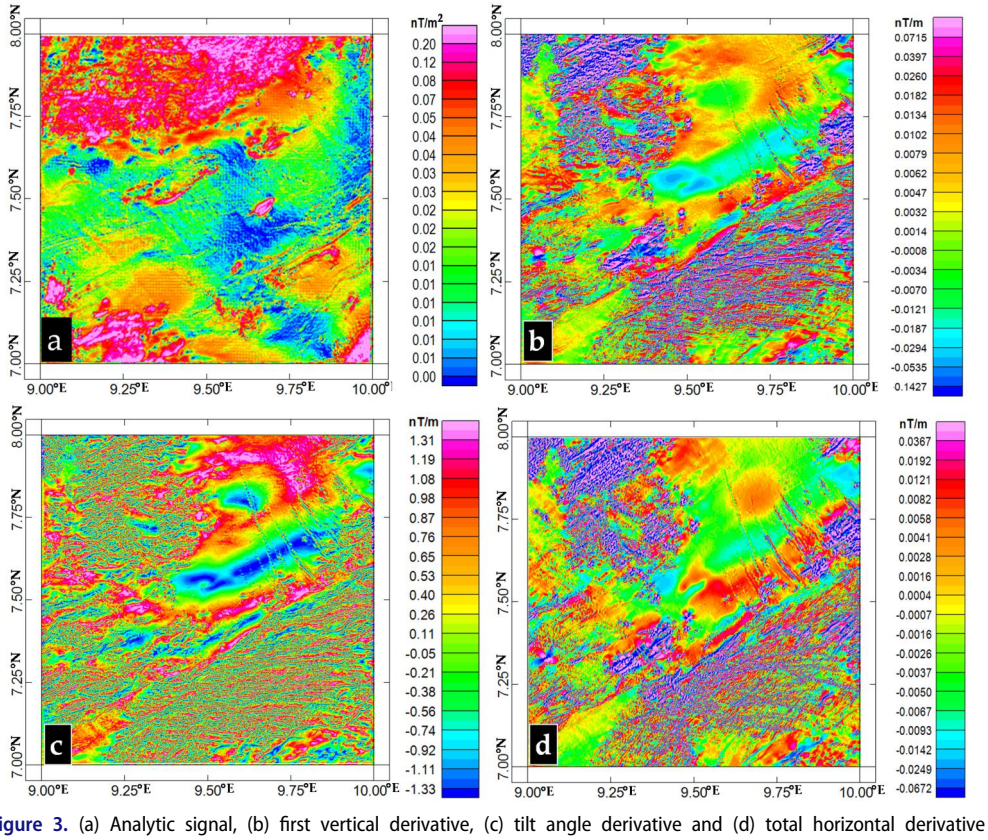

Figure 3. (a) Analytic signal, (b) first vertical derivative, (c) tilt angle derivative and (d) total horizontal derivative maps.

Calculating the FVD in magnetic data filtering is similar to directly detecting the vertical gradient with a magnetic gradiometer, magnifying shallow magnetic sources and

enhancing the resolution of the magnetic bodies (Pal and Majumdar 2015). The nth derivative is given as:

$$F(\omega) = \omega^n \tag{2}$$

The TAD is less sensitive to noise than other filtering operations that apply higher-order derivatives. It works as a marker for the borders of geologic structures that constitute magnetic anomalies. The TAD is defined as the anomalies' vertical derivative divided by their horizontal derivative. The formula is as follows:

$$\theta = \tan^{-1} = \frac{\frac{\partial^2 A}{\partial z^2}}{THD_{(x,y)}} \tag{3}$$

The THD, which is well-defined as follows, is a widely employed edge detection filter (Blakely 1995). The THD is mathematically defined as:

$$THD_{(x,y)} = \left[\left(\frac{\partial A}{\partial x}\right)^2 + \left(\frac{\partial A}{\partial y}\right)^2\right]^{\frac{1}{2}} \tag{4}$$

where $\frac{\partial T}{\partial x}$ and $\frac{\partial T}{\partial y}$ are the two orthogonal horizontal-derivatives of the magnetic data, and the magnetic anomaly is A.

The procedures involved in CET analysis comprise of structural complexity, lineation detection, texture analysis and lineation vectorization processes. These programs can be applied in a number of tasks, including grid texture analysis, edge detection, thresholding, lineament recognition and detecting structurally complex areas (Kovesi 1991; Lam et al. 1992; Kovesi 1997) (Figure 4). The exhaustive trend detection menu was developed specifically for the detection of borders in potential field data. Entropy and standard deviation

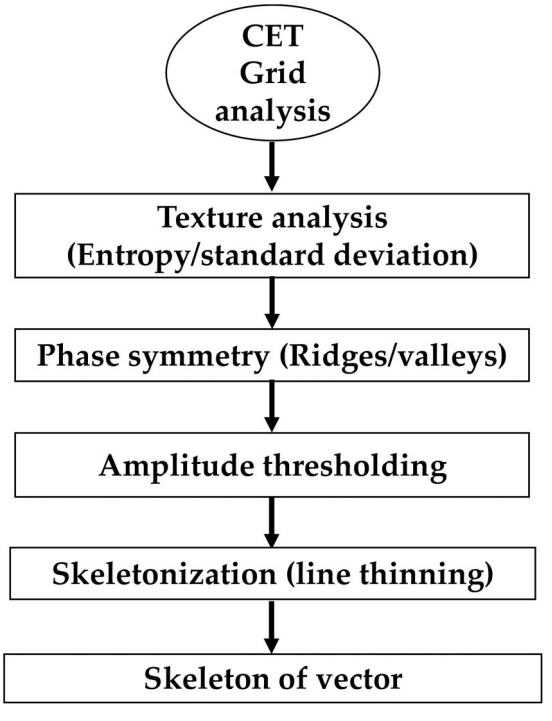

Figure 4. The flow chart of the Cet algorithm applied to magnetic data.

are two different procedures (ie ridges and edges in the texture) for approximating trends that are built-in in this menu (Kovesi 1991; Lam et al. 1992; Kovesi 1997).

In the localized windows of a dataset, the entropy plugin provides a measurement of the textural information. It quantifies the data into discrete bins in an attempt to define the total number of discrete values that resulted from that quantization (Holden et al. 2008, 2010). This analysis is applied to define the statistical randomness of neighbourhood data values. Allocated a definite number of bins, n, for a particular cell I in a k × k sized neighbourhood, for a histogram and calculate the entropy as follows (Holden et al. 2008, 2010):

$$E = -\sum_{i=1}^{n} p_i \log p_i \tag{5}$$

where the histogram of n bins has been normalized to produce the probability p.

The standard deviation offers an estimate of the local data discrepancy. For each grid cell, the standard deviation of the nearby data values is determined. When compared to the background signal, important features often display great fluctuation. For a window with N cells and a mean value of μ, the standard deviation of σ of the cell values xi is:

$$\sigma = \sqrt{\frac{1}{N}\sum_{i=1}^{N}(x_i - \mu)^2} \tag{6}$$

The SPI characteristically creates the outputs of imageries from which depth to magnetic bodies can be observed (Smith et al. 1998). Based on Smith et al. (1998), this technique analyses the qualities of the analytic signal and second vertical-derivative responses. The analysis can offer an appropriate geologic model and unlike the SED (Smith et al. 1998), the depth approximation is not dependent on any assumptions made on the geologic model. Also, it is unnecessary to subject the input grid to a reduction-to-pole procedure as the estimated depth values are non-reliant on the angle of the inclination and declination of the magnetic field. When one has a full understanding of the geology of the study location, magnetic data analysis becomes remarkably simpler (Thurston and Smith 1997). The wavelength of the ASIG is characteristically where the SPI approximations of depth come from. The ASIG based on Nabighian (1972), A_1(x, z) is given as:

$$A_1(x,z) = \frac{\partial M(x,z)}{\partial x} - j\frac{\partial M(x,z)}{\partial z} \tag{7}$$

j is the imaginary number, x and z are Cartesian coordinates for the horizontal and the vertical directions perpendicular to the strike, respectively, and M(x, z) is the magnitude of the anomalous total magnetic field,.

The Euler homogeneity equation provides apparent depth to the magnetic bodies. This technique connects the magnetic field and its gradient components to the location of the magnetic anomaly, with the degree of homogeneity described as a structural index (SI). The Euler's homogeneity equation for magnetic data can be stated as:

$$(x - x_0)\frac{\partial T}{\partial x} + (y - y_0)\frac{\partial T}{\partial y}(z - z_0)\frac{\partial T}{\partial z} = N(B - T) \tag{8}$$

where (x_0, y_0, z_0) is the location of the magnetic source whose total field (T) is observed at (x, y, z). N, a measurement of the magnetic field fall-off rate, can be taken to be the SI, and B is the local magnetic field. The method involves selecting a suitable SI value and determining the equation for the best x_0, y_0, z_0 and B by means of least-square inversion.

Furthermore, a square window size that describes the number of gridded data cells to be applied in the inversion at each chosen solution must be provided.

Two-dimensional (2-D) forward modelling using the GM-SYS tool of Oasis Montaj was employed to evaluate sediment thicknesses, map tectonic structures and basement topography. The forward modelling technique requires making a hypothetical geologic model and computing the magnetic responses centred on Talwani and Hiertzler (1964) and Talwani et al. (1959) and using the algorithms defined by Won and Bevis (1987). The gridded database for modelling was obtained from two N-S oriented profiles on the magnetic gridded data (Figure 2). The profile locations which ran perpendicular to the magnetic sources with E-W orientation, were determined after magnetic enhancement maps (Figure 3) were generated.

The radiometric data analysis involves correcting the raw data for any distortions or biases. This includes adjustments for atmospheric effects, sensor noise and angle of incidence. To eliminate any apparent residual errors concomitant with the airborne radiometric data, the grid and image tool in Geosoft® software was used and the total count images were generated after micro-levelling the whole dataset. Generally, the total count represents the sum of all detected radiation over a specific period or area and can indicate the presence of certain materials like uranium, potassium or thorium in geological surveys. Converting radiometric measurements into actionable information often involves comparing observed data to known standards or models. Analysing the variability and distribution of total counts (like potassium, thorium or uranium) can provide insights into the underlying processes that can be useful in estimating mineral concentrations. Radiometric data are generally displayed as a map, with colours signifying sample values. Usually, red areas in the maps show high gamma ray counts and the blue areas indicate low counts. A different way to display radiometric data is to join three datasets on the one picture using a red-green-blue ternary ratio. Unlike the other airborne geophysical methods, there are no mathematical models that will permit us to compute the theoretical radiometric response of a specific source (Grasty 1979). Interpretation of radiometric data is, hence, more like interpreting the results of a conventional geological survey. It is generally necessary to relate the results of geological and/or geochemical sampling with, for example, the colour patterns in a radiometric ternary map to attain a full understanding of the consequences of the map. Nevertheless, an understanding of how radiometric surveys can be employed to exploration problems needs us to consider the geological sources of radioactivity.

Results

Interpretation of short wavelength and CET maps

In order to evaluate near surface geologic features, great emphasis was laid on enhancing short wavelength anomalies of the total magnetic intensity data. Figure 3 revealed complex geological structures (represented by densely packed red to pink colour) situated at the northern, northwestern and southwestern flanks of the study area. The rocks within these segments of the study area are rich in magnetite and are considered to be responsible for the high magnetisation. These observed short wavelength structures are caused by near surface igneous intrusions and are usually related to rift mineralization (Ekwok et al. 2019). Also, the maps (Figure 3) delineated shallow and intra-basin structures (represented by yellow to red colour) that trend in the NE-SW direction. Associated with the observed anomalies are some deeper and broader structures (represented by blue colour).

These observations validate previous findings of the existence of an axial structure (attributed to the joint effects of igneous intrusions and shallow basement) bordered by elongated sedimentary troughs in the Benue Trough (Ofoegbu 1983, 1984a, 1984b; Ofoegbu and Mohan 1990; Ofoegbu and Onuoha 1991).

The CET lineation maps (Figure 5(a–d)) resulting from the ASIG, FVD, TAD and THD data (Figure 3(a–d)) were respectively used to produce the geologic structural maps. The analysis eventually resulted in the generation of comprehensive structural maps, which are very valuable for mineral investigations. The CET lineation map (Figure 5(a)) obtained from the ASIG magnetic grid (Figure 3(a)) displayed a predominant NE-SW structural trend with minor NNE-SSW orientation of lineation. Figure 5(b) displays the geologic structural map of the CET applied on the FVD grid (Figure 3(b)). The structural orientation within the study location trends generally in the NE-SW direction with minor E-W orientation. In addition, the application of the CET on the TAD (Figure 3(c)), shows major and minor geologic structural trends of NE-SW and NNE-SSW and E-W (Figure 5(c)), respectively. Likewise, the CET-generated structural map (Figure 5(d)) from the THD grid (Figure 3(d)) indicates major and minor trends in NE-SW and E-W directions,

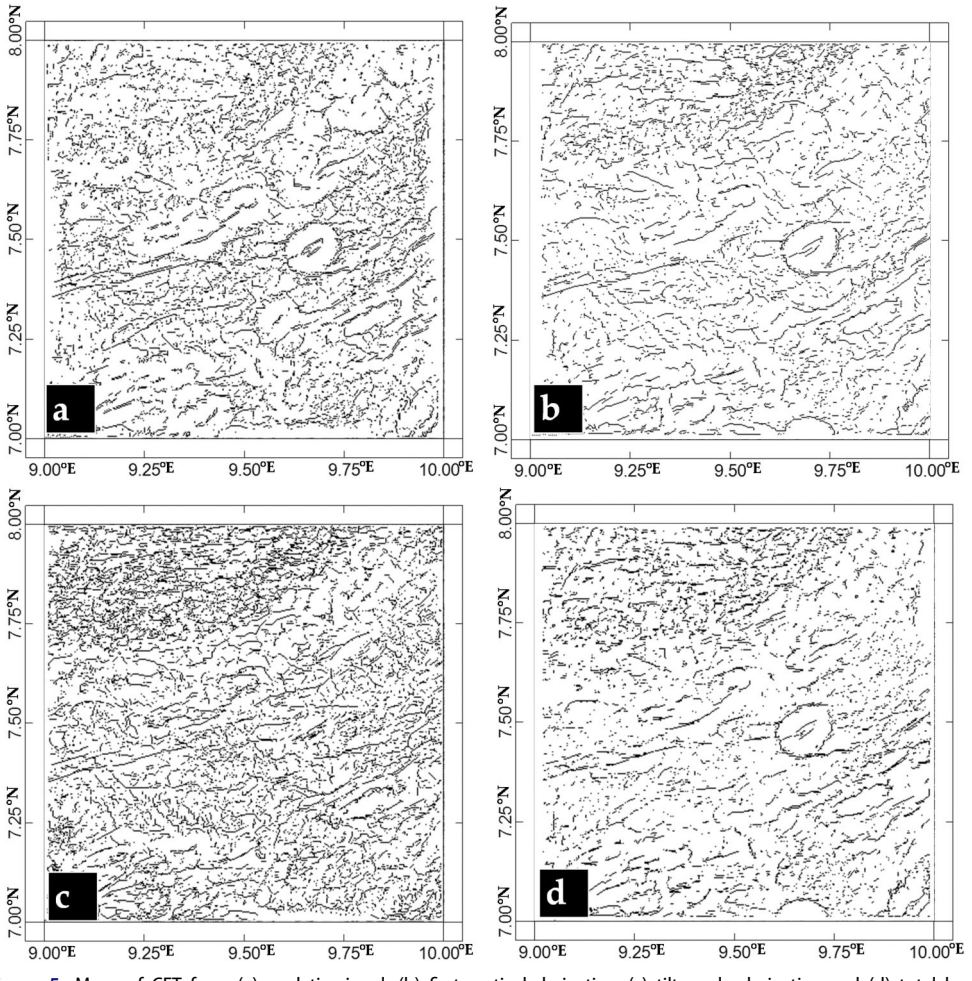

Figure 5. Maps of CET from (a) analytic signal, (b) first vertical derivative, (c) tilt angle derivative and (d) total horizontal derivative grids.

respectively. In general, an oval-shaped geologic structure situated towards the eastern end of the investigated area was mapped by the CET-generated structural maps from the ASIG, FVD and THD grids (Figure 5(a,b, d)). This is suspected to be post-depositional igneous intrusions in the MBT (Ofoegbu 1984a; Ofoegbu and Mohan 1990; Ofoegbu and Onuoha 1991) that are cylindrically shaped. The placement of this structure in this study area matches the placement of an anticline on the geologic map (Figure 1). In general, the leading geologic structural orientation of NE-SW revealed by the rose petals (Figure 6) denotes the regional strike direction reported by previous studies (Ekwok, Achadu, et al., 2022; Ekwok, Akpan, Achadu, and Ulem, 2022; Ekwok, Eldosouky, Achadu, et al. 2022). The rifting of the African Plate in the Cretaceous (Ajayi 1976; Ajayi et al. 2008) initiated the dominant NE-SW regional structural trend (Nwankwo and Ekine 2009) that is detected. The observed clusters and complex pattern of the structural maps (Figure 5) reflect polyphase distortions of the MBT triggered by post-depositional tectonic activities in the Neogene (Ofoegbu 1984a; Ofoegbu and Mohan 1990; Ofoegbu and Onuoha 1991). These igneous-related distortions in the MBT have created different geologic structures, like folds, faults, unconformities and shear zones, which have influenced

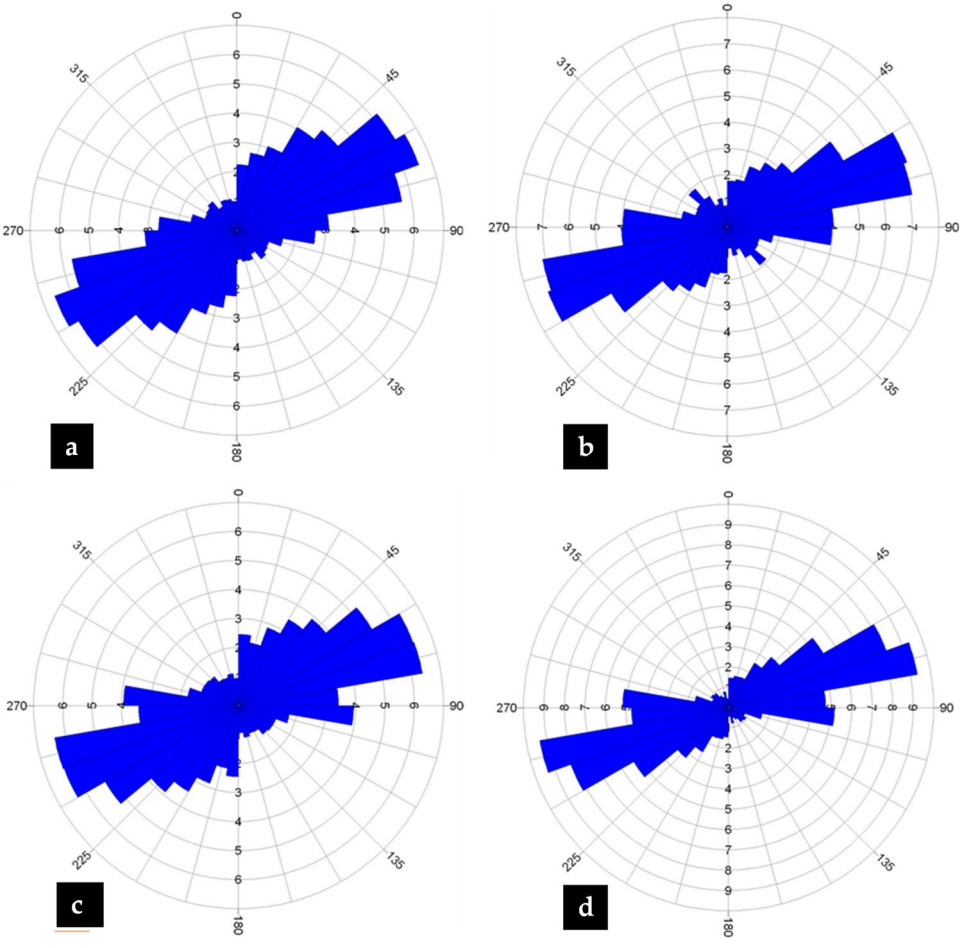

Figure 6. Rose diagrams of CET generated structural maps from (a) analytic signal, (b) first vertical derivative, (c) tilt angle derivative and (d) total horizontal derivative.

the geometry of the rocks (Ajibade et al., 1987; Ekwok, Achadu, et al., 2022; Ekwok, Akpan, Achadu, and Ulem, 2022).

Interpretation of radiometric maps

Gamma-rays released from the surface of the Earth relate with the mineralogy and geochemistry of soils, saprolite, colluvial and alluvial sediments (Boadi et al. 2013). Suitable knowledge of the responses from regolith and bedrock has proven to be invaluable in understanding geomorphic processes and mapping regoliths (Wilford et al. 1997). The distribution and concentration of radioelements are commonly altered by weathering (Ekwok, Akpan, Achadu, et al. 2021).

The potassium map (Figure 7(a)) displays diverse potassium concentration levels that coincide with various lithological units and variations in the research area. The main source of potassium radiation is granite, or felsic igneous rock, which is rich in potash feldspars (Gunn et al. 1997). Basalts and andesite, or mafic rocks, have modest concentrations of K (Gunn et al. 1997). Also, alterations in the rock may cause an increase in potassium concentrations (Wilford et al. 1997). Potassic clays (illite) being the only exception, K, which is extremely soluble in weathering conditions, degenerates with increased weathering (Ramadass et al. 2015). The colours red-pink, orange-yellow and blue in Figure 7(a) indicate high, intermediate and low potassium intensities, respectively. The high concentration (red-pink colour) is thought to have emanated from shales, illite and

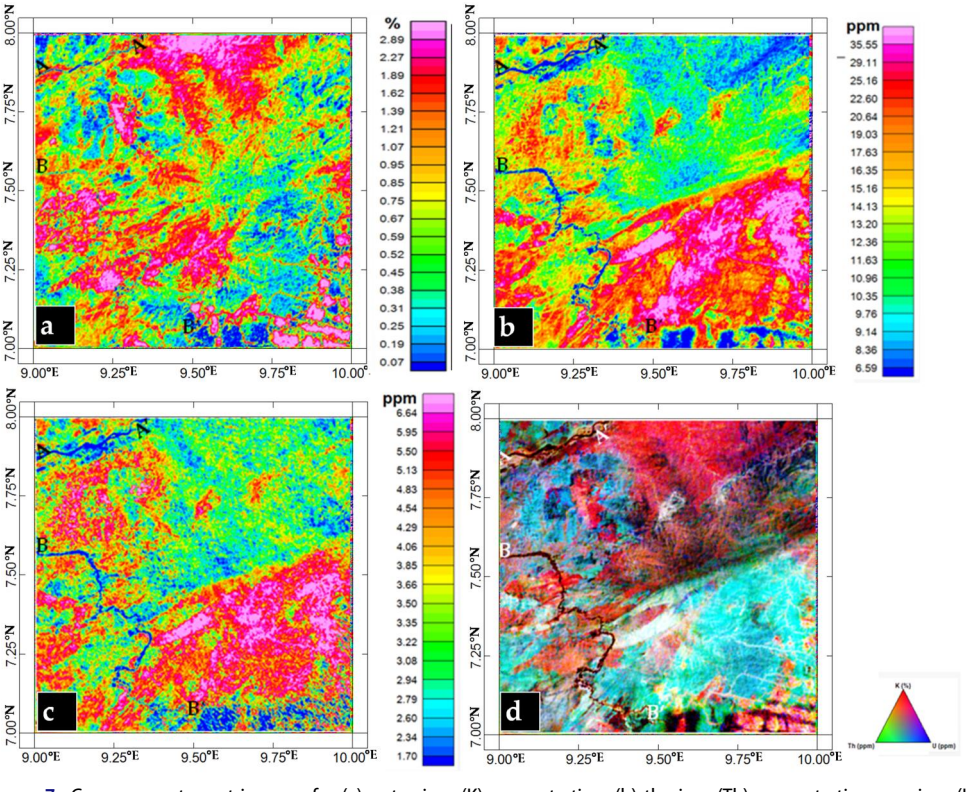

Figure 7. Gamma spectrometric maps for (a) potassium (K) concentration, (b) thorium (Th) concentration, uranium (U) concentration and (d) ternary image.

post-depositional igneous intrusions (like granite, pumice, obsidian, gneiss, pegmatite, greisen, schist, hornfels, slate, etc.) in the Benue Trough (Ofoegbu and Mohan 1990; Ofoegbu and Onuoha 1991). The low-concentration portions (blue colour) match with the locations of basalts (since they are known to have low K concentrations) and areas with chalky or peaty soils (Gunn et al. 1997). Potassium deficiency in sediments can also be caused by low soil pH, high calcium concentration, extreme liming, or lack of soil oxygen (Gunn et al. 1997). Low Th concentration (Figure 7(b)) dominantly occurred at the central, northern and northeastern portions of the investigated area. These areas of low Th concentration (blue colour) suggest lithologic borders, mafic minerals, altered patterns in distinct rocks or shears and faults that hosted hydrothermal fluid that leached Th (Boadi et al. 2013; Ekwok, Akpan, Achadu, et al. 2021). High Th concentrations are detected in the southwest, southern and southeastern flanks, indicating the prevalence of felsic minerals (Boadi et al. 2013). The high concentration of Th in the Benue Trough was reported by Ekwok, Akpan, Achadu, et al. (2021) it is mostly caused by shale, alluvium and other highly weathered colluvial sediments deposited in the lowlands.

The high and low Uranium (U) (Figure 7(c)) geographical distribution closely matches that observed in Figure 7(b). In terms of locating the granitoid rocks in the investigated area, the map depicts good characterization. While the western and northwestern portions of the investigated area are dominated by an intermediate intensity (orange-yellow) with some scanty high U content, the central, northern and northeastern areas display low U concentration described with blue colour. High U content (reddish-pink) predominates in the southern and southeastern flanks. The hydrothermal fluid linked to post-depositional granitic intrusions (Dill et al. 2010; Mineral Resources of the Western US 2017) and associated rock alterations, oxides, residual clay and accessory minerals (Wilford et al. 1997) that are believed to be the cause of this high U content.

The colours red, green and blue, respectively, define the collective intensities of the K, Th and U concentrations on the ternary map (Figure 7(d)). Figure 7(d) shows a relatively good correlation with the geology of the study area (Figure 1). High K content is revealed by the granitoids or mafic rocks (with associated hydrothermal solutions) in the northern and northeastern segments of the investigated area. These rocks are located in the vicinity where there exist lithologic boundaries, faults, fractures and other locations where silicification and other hydrothermal alterations are intense (Boadi et al. 2013). A green zone (high Th concentration) dominates the southern and southeastern parts, while the remaining portions of the area have an inconsistent distribution of K, Th and U with no single radiometric element clearly dominating. The diffuse lithological borders (Figure 7(a–c)) which are situated at the northwestern and southwestern flanks (and represented by AA' and BB', respectively) of the area were very prominent in the ternary map (Figure 7(d)). The northwestern border coincides with the location of granitic gneiss boundary with migmatite, while southwestern frontier is relatively near the boundary between alluvium and shale, siltstone or sandstone (and somewhat nearby to the location of a stream channel (Figure 1)).

Interpretation of 2D magnetic models, SPI and SED maps

Models developed from the two profiles (Figure 2) are presented as Figures 8 and 9. Figure 8 curve is centrally jagged representing igneous intrusions characterized by a susceptibility of 0.005501. This intrusion is flanked by Precambrian crustal blocks with susceptibility of 0.003701 (left) and 0.003051 (left). The somewhat serrated pattern of

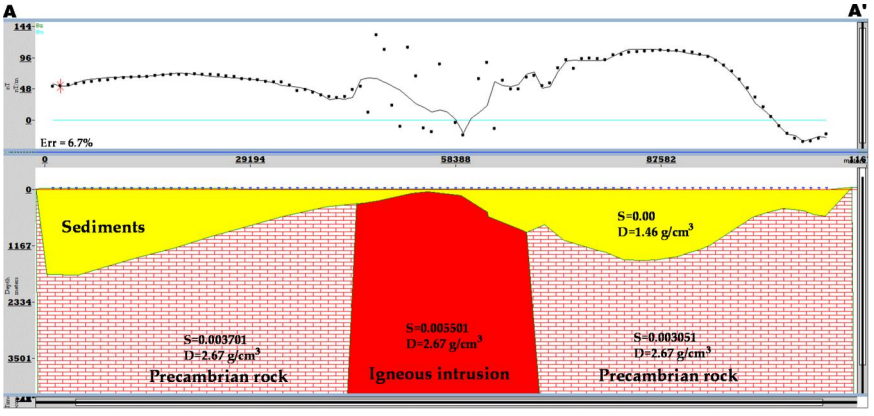

Figure 8. 2D magnetic model of profile 1.

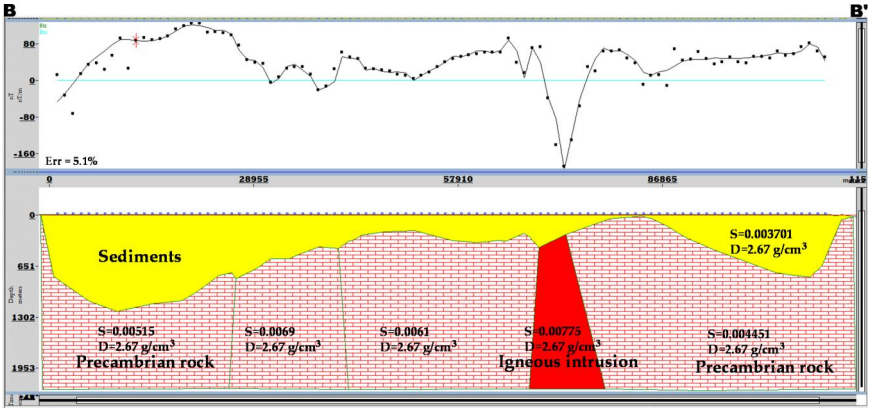

Figure 9. 2D magnetic model of profile 2.

Figure 9 curve has igneous with susceptibility of 0.00775. Other crustal blocks have susceptibility values of 0.00515, 0.0069, 0.0061 and 0.004451. The observed serrated nature of Figure 9 is suspected to be influenced by tectonic event. The intrusions and Precambrian basement are capped sediments generally less than 1500 m.

The SPI and SED procedures were applied to assess the spatial distribution of magnetic bodies and their related depth. These techniques are suitable for outlining isolated as well as multiple magnetic source geometries (Telford et al. 1990). The SPI (Figure 10(a)) depth to shallow and deep magnetic bodies ranged from ∼59.69 to ∼145.35 m (pink-yellow) and ∼145.35 to ∼1414.33 m (lemon green-blue), respectively. Likewise, the SED (Figure 10(b)) displays depth values of ∼9.12 to ∼216.66 m (blue-lemon green) and ∼231.31 to ∼1326.46 m (yellow-pink) for shallow and deep magnetic bodies, respectively. The SPI colour legend bar is defined by a negative sign indicating depth calculation from the surface of the Earth downward (Thurston et al. 2000). The observed results (Figure 10), the northwestern and the southeastern flanks are dominated by thin sedimentation. The northwestern portion of the area is controlled by porphyritic granite and granitic gneiss (Figure 1) while the southeastern portion is occupied by metasedimentary rocks. On the whole, Figure 10 thick sedimentation exists around the central area and runs laterally in the NE direction.

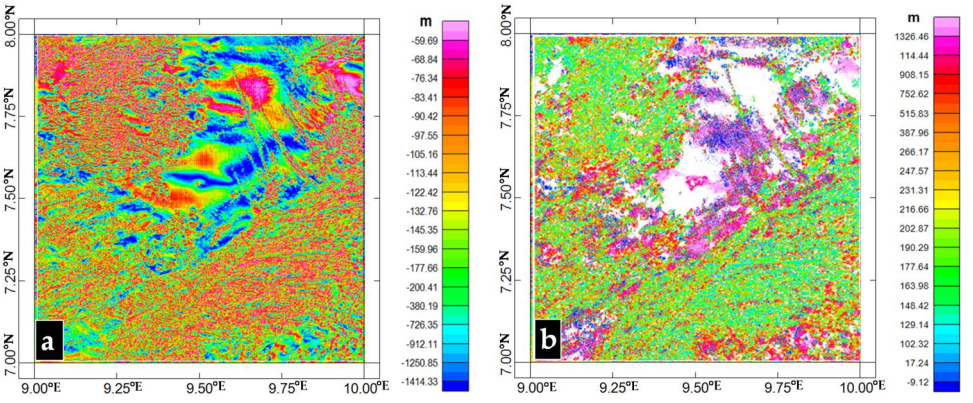

Figure 10. Maps of (a) source parameter imaging and (b) standard Euler deconvolution.

Discussion

An integrated geophysical interpretation involving magnetic and radiometric data for polymetallic-magmatic hydrothermal minerals have been carried out (Airo 2002; Wemegah et al. 2015). Massive sulphide, base metals, shear-hosted gold and a lot of other deposit sorts are normally connected with modifications relating to potassium feldspar in volcanic regions (Offler and Whitford 1992; Dill et al. 2013). The MBT has witnessed post-depositional tectonic episodes in the Neogene that generated several faults, folds and unconformities (Ajayi et al. 2008). Also, these events created hydrothermal alteration regions (Ekwok, Akpan, and Kudamnya 2020) and generated brine fields from igneous-related hydrothermal fluid (Ekwok, Akpan, Achadu, Thompson, et al. 2022).

Recently, high precision edge detection methods like the tilt angle of total horizontal gradient, the softsign function, and the improved logistic function were applied in the Lower Benue Trough. Delineated geologic structures trend in the NE–SW, NW–SE, NNE–SSW and NNW–SSE directions (Ekwok, Eldosouky, Ben, et al. 2022). Also, the orientations of geologic structures mapped in the Southeast region of Nigeria indicated trend in the NE–SW, NNE–SSW, N–S, E–W and NW–SE directions (Eldosouky et al. 2022). Similarly, research by Ekwok, Achadu, et al. (2022) carried in the Obudu Basement Plateau and Abakaliki Anticlinorium using both simulated and real data showed major geologic structures trend of NW and NE, as well as minor NS directions. Recent research in the Obudu Basement Complex involving the CET mapped geologic structures that trend in the NE–SW, NNE–SSW, E–W and N–S directions (Ekwok et al. 2024). In addition, the same study showed the dominant geologic structural orientations of NE–SW and NNE–SSW reflect the regional strike orientation. Furthermore, the engagement of the CET analysis has enabled the comprehensive delineation of geologic structures and the mapping of favourable exploration targets in the MBT. The structural maps (Figure 5) of CET obtained from ASIG, FVD, TAD and THD gridded data correlate strongly with each other. The observed NE-SW dominant structural orientation (Figure 6) indicates the regional strike trend of the Benue Trough which is interrelated to the Cretaceous rifting of the African Plate (Ajayi 1976; Ajayi et al. 2008; Nwankwo and Ekine 2009). The extensive post-depositional tectonic events in the Neogene (Ofoegbu 1984a; Ofoegbu and Mohan 1990; Ofoegbu and Onuoha 1991) caused polyphase distortions and generation of clusters and complex patterns of geologic structures (Figure 5). Hydrothermal and structural control associated with igneous intrusions are generally connected with mineralization (Dill et al. 2013). It has been reported that polymetallic minerals including uranium,

copper, gold, lead, zinc and brines in rift environments, such as the Benue Trough are linked to deep-seated granite pluton (Gandhi et al. 1996; Mineral Resources of the Western US 2017; Ekwok et al. 2019).

The spatial dissemination and placement of the radiometric anomalies from the potassium, thorium and uranium concentrations correlate fairly with each other (Figure 7). Figure 7(d) reveals noticeably the sub-geologic regions, high potassium and uranium concentrations plus the diffuse lithological boundaries positioned at the northwestern and southwestern parts and marked as AA' and BB', respectively. The northwestern flank coincides with the location of granitic gneiss dominated by migmatite, while the southwestern part is dominated by alluvium, shale, siltstone, or sandstone. On the whole, hydrothermal rock modifications, felsic rocks and related minerals, the widespread shale, oxides, residual clay and accessory minerals are the major sources of high potassium, thorium and uranium concentrations detected in the investigated area.

Figure 11 connects the co-occurrence of high magnetization and potassium concentration between the analytic signal and the potassium and ternary maps. The region with corresponding high magnetization and potassium concentration was noted using arrow lines amongst the maps. Such regions with coexistent high potassium and magnetization indicate a high potential for polymetallic-magnetic mineralization (Geological Survey of Canada 1992; Schroeter 1995; Bierlein et al. 1996; Dill et al. 2013).

The MBT which is a fragment of the Benue Trough has been described as a region that has experienced polyphase tectonic events (Cratchley and Jones 1965; Ofoegbu 1984a, 1984b; Ofoegbu and Mohan 1990; Ofoegbu and Onuoha 1991). From several published investigations that applied different geophysical and depth estimation methods, depth solutions within the Benue Trough were reported in the range of 1500–12,000 m (Burke et al. 1971; Ajayi 1976; Ofoegbu 1984a, 1984b; Reijers and Petters 1987; Ofoegbu and Mohan 1990; Ekwok et al. 2019; etc.). The tilt depth method revealed depth to geological contacts and basement in the range of ~500 to ~5000 m in the Lower Benue Trough (Eldosouky et al. 2022). Likewise, the depths of about 0–2100 m were observed in Ogoja region dominated by Santonian intrusions related to the Abakaliki Anticlinorium (Ekwok,

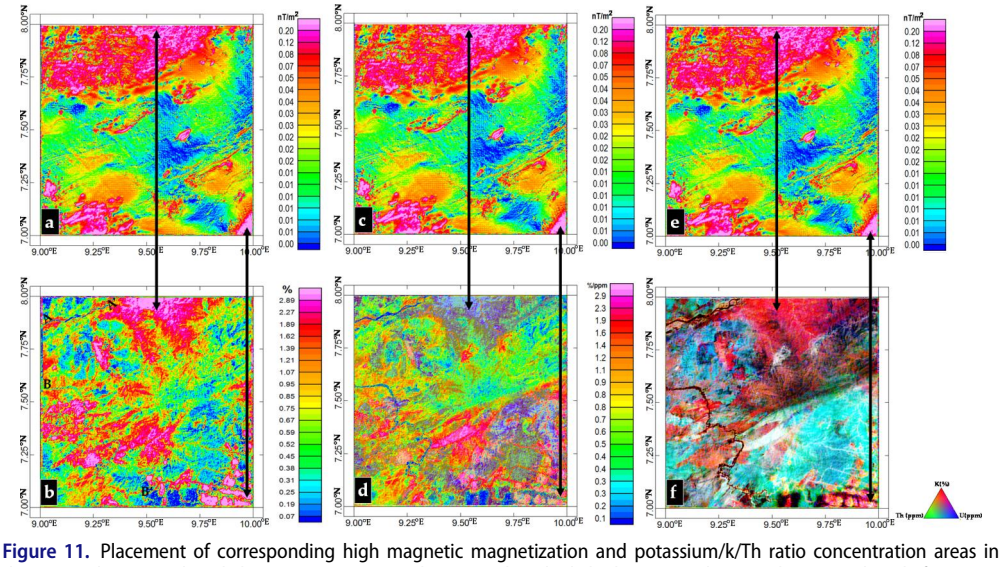

Figure 11. Placement of corresponding high magnetic magnetization and potassium/k/Th ratio concentration areas in the (a) analytic signal and (b) potassium, (c) analytic signal and (d) k/Th ratio and (e) analytic signal and (f) ternary maps.

Eldosouky, Ben, et al. 2022). On the other hand, depth range of approximately 286 to 5974 m involving depth determination methods like source parameter imaging, standard Euler deconvolution and 2D modelling in the Upper Benue Trough have been reported (Ekwok, Achadu, et al., 2022). In the study area, the depth values observed from the 2D models, SPI and SED (Figures 8, 9 and 10) which strongly correlate with each other, indicate depth to basement of largely <1500 m. The observed thin sedimentation is caused by the extensive occurrence of porphyritic granite, granitic gneiss and metasedimentary rocks (Figure 1) (Ajayi 1976; Ajayi et al. 2008; Obaje 2009). Furthermore, the observed complex geologic structures (Figure 5) are triggered by post-depositional intrusions mapped by the 2D models (Figures 8 and 9). These intrusions caused the baking, doming and fracturing of the overlying sediments (Ekwok, Akpan, Kudamnya, and Ebong 2020). The igneous-related hydrothermal fluids and associated dissolved minerals (like gold, copper, lead and zinc) migrate and accumulate in these openings (Dill et al. 2010, 2013; Mineral Resources of the Western US 2017).

Conclusion

In this study, the CET method was applied on the enhanced total magnetic intensity data involving ASIG, FVD, TAD and THD. The CET-derived structural maps involving various enhancement filters show a strong correlation with each other. It was noticed that the geologic structures were dominantly oriented in the NE-SW direction with minor NNE-SSW and E-W trends. The main NE-SW orientation indicates the major strike direction of the Benue Trough, reflecting the regional strike of lineament linked to the Cretaceous rifting of the African Plate. Radiometric maps delineated clearly high intensities of potassium, thorium and uranium concentrations. The associated anomalies are indicative of widespread shales, felsic minerals, residual clay, oxides and accessory minerals as well as the altered hydrothermal rocks that constitute the regolith of the investigated area. The equivalent high intensity of the analytic signal with potassium and ternary maps is a possible site for polymetallic-magmatic hydrothermal mineralization. Furthermore, igneous intrusions that caused the complex geologic structural pattern, baking and doming of sediments were delineated by the 2D forward models. Depth to basement involving SPI, SED and 2D modelling methods in the investigated area was observed to be <1500 m. In general, the joint magnetic and radiometric data created a relationship between geologic structures, lithology and hydrothermal modification configurations. The relationship demonstrates that the hydrothermal systems are structurally controlled and not restricted to any specific geologic region. Generally, the observed near-surface geologic structures serve as the migration paths and accumulation zones for hydrothermal minerals associated with igneous intrusions and rifting.

Generally, lineaments trend in the NE-WS, NNE-SSW, NW-SE and E-W directions. The high magnetic contrast between rocks along contacts indicates a potential pathway for hydrothermal fluid migration and mineralization. Also, the tilt angle derivative map showed a centrally placed deep-seated weak zone that trends in somewhat E-W direction. Furthermore, the main sources of magnetism and anticlinal structures in the MBT were detected with the aid of an analytic signal map. Gamma spectrometric imageries mapped distinctly high potassium, thorium and uranium concentration zones. These radiometric anomalies are caused by felsic minerals, hydrothermal rock alterations, widespread shale, residual clay, oxides and accessory minerals that constitute the regolith of the area. The geologic map of the study area seems inappropriate. However, the ternary map highlighted clearly the various lithological regions and boundaries. The coincident high

magnetic and potassium intensities sites within the study area are feasible locations for polymetallic-magmatic hydrothermal deposits. Generally, the combined magnetic and radiometric dataset established connections between lithology, geologic structures and hydrothermal alteration patterns. The relationship demonstrates that the hydrothermal systems are structurally controlled and not restricted to any specific geologic region.

Author contributions

S.E.E., Conceptualization, methodology, data, processing, writing, original draft preparation. A.M.G., Validation, methodology. A.A.O., methodology, reviewing and editing, S.I.U., Validation, conceptualization. M.I.M., Methodology, investigation. K.A., Funding acquisition, review & editing. P.A., review & editing. A.E.A., review & editing. A.M.E., Methodology, reviewing and editing, conceptualization. All authors have read and agreed to the published version of the manuscript.

Disclosure statement

No potential conflict of interest was reported by the author(s).

Funding

This wok was supported by Researchers Supporting Project number (RSP2024R351), King Saud University, Riyadh, Saudi Arabia.

ORCID

Ahmed M. Eldosouky http://orcid.org/0000-0003-1928-9775

Data availability statement

The data used in this study can be made available upon request to the corresponding author (Dr. Ahmed M. Eldosouky).

References

Abdelrahman EM, Ammar AA, Hassanein HIE, Soliman KS. 2006. Separation of anomalous aerial radiospectrometric zones using least-squares method on a sample area in Egypt. Arab J Sci Eng. 32(1A): 19–35.

Abdelrahman K, Ekwok SE, Ulem CA, Eldosouky AM, Al-Otaibi N, Hazaea BY, Hazaea SA, Andráš P, Akpan AE. 2023. Exploratory mapping of the geothermal anomalies in the Neoproterozoic Arabian Shield, Saudi Arabia, using magnetic data. Minerals. 13(5):694. doi: 10.3390/min13050694.

Adekeye J, Yakubu B. 2016. Geophysical investigation of the basement complex rocks in parts of Kogi State, North Central Nigeria. J Appl Geol Geophys. 4(1):43–52.

Adeyemo I, Bolarinwa S, Fagbohun B, Ogunlana A, Adeleke A. 2018. Integration of magnetic and gravity methods for hydrocarbon exploration in the Gongola Basin, Northeast Nigeria. J Afr Earth Sci. 145: 165–177.

Airo ML. 2002. Aeromagnetic and aeroradiometric response to hydrothermal alteration. Surv Geophys. 23(4):273–302. doi: 10.1023/A:1015556614694.

Ajakaiye DE. 1976. The geology of the Benue valley and adjacent areas. In: Kogbe CA, editor. Geology of Nigeria. Elizabethan Publishing Company; p. 379–400.

Ajayi CO. 1976. The geology of the Benue valley and adjacent areas. In: Kogbe CA, editor. Geology of Nigeria. Elizabethan Publishing Company; p. 379–400.

Ajayi CO, Tse TG, Ojo OJ. 2008. Tectonic evolution of the middle Benue trough (Nigeria). J Afr Earth Sci. 52(4-5):153–165.

Ajibade AC, Woakes M, Rahaman MA. 1987. Proterozoic crustal development in the Pan-African Regime of Nigeria. Proterozic Lithospheric Evolution. 17:259–271.
Akpan AE, Ebong DE, Ekwok SE, Joseph S. 2014. Geophysical and geological studies of the spread and industrial quality of Okurike Barite deposit. Am J Environ Sci. 10(6):566–574. doi: 10.3844/ajessp.2014.566.574.
Alfaifi HJ, Ekwok SE, Ulem CA, Eldosouky AM, Qaysi S, Abdelrahman k, Andráš P, Akpan AE., 2023. Exploratory assessment of geothermal resources in some parts of the Middle Benue Trough of Nigeria using airborne potential field data. J King Saud Univ Sci. 35(2):102521. doi: 10.1016/j.jksus.2022.102521.
Anudu GK, Stephenson RA, Ofoegbu CO, Obrike SE. 2020. Basement morphology of the middle Benue Trough, Nigeria, revealed from analysis of high-resolution aeromagnetic data using grid-based operator methods. J Afr Earth Sci. 162:103724. doi: 10.1016/j.jafrearsci.2019.103724.
Araujo V, Santos E, Santos J, Costa F, Amarante J. 2019. Application of airborne radiometric survey to uranium exploration in the Coimbra region, central Portugal. J Environ Radioact. 196:42–52.
Arora K, Rawat G, Srikumar V. 2019. Integrated interpretation of airborne magnetic and radiometric data for delineation of uranium mineralization in the western part of Singhbhum Shear Zone, India. J Appl Geophys. 160:100–113.
Ayodele K, Ayolabi E, Olayinka A, Olawepo A, Olayiwola M. 2018. Geological and geophysical investigation of the Igarra area, southwestern Nigeria: an integrated approach. J Afr Earth Sci. 138:240–253.
Beckett KA. 2003. 2003. Airborne geophysics applied to groundwater modelling. In: Roach IC, editor. Advances in regolith. p. 8–10.
Ben UC, Ekwok SE, Akpan AE, Mbonu CC, Eldosouky AM, Abdelrahman K, Gómez-Ortiz D. 2022. Interpretation of magnetic anomalies by simple geometrical structures using the manta-ray foraging optimization. Front Earth Sci. 10:849079. doi: 10.3389/feart.2022.849079.
Ben UC, Mbonu CC, Thompson CE, Ekwok SE, Akpan AE, Akpabio I, Eldosouky AM, Abdelrahman K, Alzahrani H, Gómez-Ortiz D, et al. 2023. Investigating the applicability of the social spider optimization for the inversion of magnetic anomalies caused by dykes. J King Saud Univ Sci. 35(3):102569. doi: 10.1016/j.jksus.2023.102569.
Benkhelil J. 1987. The origin and evolution of the Cretaceous Benue Trough (Nigeria). J Afr Earth Sci. 8(2-4):251–282. doi: 10.1016/S0899-5362(89)80028-4.
Bierlein FP, Ashley PM, Seccombe PK. 1996. Origin of hydrothermal Cu-Zn-Pb mineralisation in the Olary Block, South Australia: evidence from fluid inclusions and sulphur isotopes. Precambrian Res. 79(3-4):281–305. doi: 10.1016/0301-9268(95)00098-4.
Blakely RJ. 1995. Potential theory in gravity and magnetic applications. Cambridge: Cambridge University Press.
Blinman E, Cudahy T, Bastrakov E. 2018. Radiometric mapping as a tool for mineral exploration in regolith-dominated terrains: a case study from the Lachlan Fold Belt, New South Wales, Australia. Ore Geol Rev. 101:733–745.
Boadi B, Wemegah DD, Preko K. 2013. Geological and structural interpretation of the Konongo area of the Ashanti gold belt of Ghana from aeromagnetic and radiometric data. Int Res J Geol Mining. 3(3):124–135.
Burk K, Dewey JF. 1974. Two plates in Africa during the Cretaceous? Nature. 249(5455):313–316., doi: 10.1038/249313a0.
Burke KCA, Dessauvagie TFW, Whiteman AJ. 1971. Opening of the gulf of Guinea and geological history of the Benue Depression and Niger delta. Nature. 233(38):51–55. doi: 10.1038/physci233051a0.
Carruth WR. 2011. Geological setting, mineralogy, and geochemistry of the lead-zinc- barite- fluorite deposits in the lower Benue Trough, southeastern Nigeria. Ore Geol Rev. 43(1):595–614.
Cratchley CR, Jones JP. 1965. An interpretation of the geology and gravity anomalies of the Benue Valley, Nigeria. Overseas Geol Surv Geophys Pap. 1:26.
Dare EO, Adekoya JA, Akintola AI. 2017. Integrated analysis of aeromagnetic and radiometric data for the determination of basement depth in parts of northeastern Nigeria. J Afr Earth Sci. 134:60–68.
Dentith M, Mudge S. 2014. Geophysics for the mineral exploration geoscientist. Cambridge University Press.
Dill HG, Botz R, Berner Z, Abdullah MB, Hamad A. 2010. The origin of pre- and synrift, hypogene Fe-P mineralization during the Cenozoic along the Dead Sea Transform Fault, Northwest Jordan. Econ Geol. 105(7):1301–1319. doi: 10.2113/econgeo.105.7.1301.
Dill HG, Garrido MM, Melcher F, Gomez MC, Weber B, Luna LI, Bahr A. 2013. Sulfidic and non-sulfidic indium mineralization of the epithermal Au–Cu–Zn–Pb–Ag deposit San Roque (Provincia Rio Negro,

SE Argentina)-with special reference to the "indium window" in zinc sulfide. Ore Geol Rev. 51:103–128. doi: 10.1016/j.oregeorev.2012.12.005.
Ebbing J, Ravenscroft P, Korte M, Hammer M. 2019. Introduction to geophysics for environmental applications. Springer.
Ekwok SE, Achadu OIM, Akpan AE, Eldosouky AM, Ufuafuonye CH, Abdelrahman K, Gómez-Ortiz D. 2022. Depth estimation of sedimentary sections and basement rocks in the Bornu Basin, Northeast Nigeria using high- resolution airborne magnetic data. Minerals. 12(3):285. doi: 10.3390/min12030285.
Ekwok SE, Akpan AE, Achadu OIM, Eze OE. 2021. Structural and lithological interpretation of aero-geophysical data in parts of the Lower Benue Trough and Obudu Plateau, Southeast Nigeria. Adv Space Res. 68(7):2841–2854. doi: 10.1016/j.asr.2021.05.019.
Ekwok SE, Akpan AE, Achadu O-IM, Thompson CE, Eldosouky AM, Abdelrahman K, András P. 2022. Towards understanding the source of brine mineralization in Southeast Nigeria: evidence from high-resolution airborne magnetic and gravity data. Minerals. 12(2):146. doi: 10.3390/min12020146.
Ekwok SE, Akpan AE, Achadu OIM, Ulem CA. 2022. Implications of tectonic anomalies from potential field data in some parts of Southeast Nigeria. Environ Earth Sci. 81(1):1–15. doi: 10.1007/s12665-021-10060-7.
Ekwok SE, Akpan AE, Ebong DE. 2019. Enhancement and modelling of aeromagnetic data of some inland basins, southeastern Nigeria. J Afr Earth Sci. 155:43–53. doi: 10.1016/j.jafrearsci.2019.02.030.
Ekwok SE, Akpan AE, Ebong ED. 2021. Assessment of crustal structures by gravity and magnetic methods in the Calabar Flank and adjoining areas of Southeastern Nigeria-a case study. Arab J Geosci. 14(4): 1–10. doi: 10.1007/s12517-021-06696-1.
Ekwok SE, Akpan AE, Ebong ED, Eze OE. 2021. Assessment of depth to magnetic sources using high resolution aeromagnetic data of some parts of the Lower Benue Trough and adjoining areas, Southeast Nigeria. Adv Space Res. 67(7):2104–2119. doi: 10.1016/j.asr.2021.01.007.
Ekwok SE, Akpan AE, Kudamnya EA. 2020. Exploratory mapping of structures controlling mineralization in Southeast Nigeria using high resolution airborne magnetic data. J Afr Earth Sci. doi: 10.1016/j.jafrearsci.2019.103700.
Ekwok SE, Akpan AE, Kudamnya EA, Ebong DE. 2020. Assessment of groundwater potential using geophysical data: a case study in parts of Cross River State, south-eastern Nigeria. Appl Water Sci. 10(6): 144. doi: 10.1007/s13201-020-01224-0.
Ekwok SE, Eldosouky AM, Achadu OIM, Akpan AE, Pham LT, Abdelrahman K, Gómez-Ortiz D, Ben UC, Fnais MS. 2022. Application of the enhanced horizontal gradient amplitude (EHGA) filter in mapping of geological structures involving magnetic data in southeast Nigeria. J King Saud Univ Sci. 34(8): 102288. doi: 10.1016/j.jksus.2022.102288.
Ekwok SE, Eldosouky AM, Ben UC, Alzahrani H, Abdelrahman K, Achadu O-IM, Pham LT, Akpan AE, Gómez-Ortiz D. 2022. Application of high-precision filters on airborne magnetic data: a case study of the Ogoja Region, Southeast Nigeria. Minerals. 12(10):1227. doi: 10.3390/min12101227.
Ekwok SE, Eldosouky AM, Essa KS, George AM, Abdelrahman K, Fnais MS, András P, Akaerue EI, Akpan AE. 2023. Particle swarm optimization (PSO) of high-quality magnetic data of the Obudu Basement Complex, Nigeria. Minerals. 13(9):1209. doi: 10.3390/min13091209.
Ekwok SE, Eldosuoky AM, Thompson EA, Ojong RA, George AM, Alarifi SS, Kharbish S, András P, Akpan AE. 2024. Mapping of geological structures and sediment thickness from analysis of aeromagnetic data over the Obudu Basement Complex of Nigeria. J Geophys Eng. 21(2):413–425. doi: 10.1093/jge/gxae012.
Eldosouky AM, Ekwok SE, Akpan AE, Achadu OIM, Pham LT, Abdelrahman K, Gómez-Ortiz D, Alarifi SS. 2022. Delineation of structural lineaments of Southeast Nigeria using high resolution aeromagnetic data. Open Geosci. 14(1):331–340. doi: 10.1515/geo-2022-0360.
Eldosouky AM, Ekwok SE, Ben UC, Ulem CA, Abdelrahman K, Gomez-Ortiz D, Akpan AE, George AM, Pham LT. 2023. Appraisal of geothermal potentials of some parts of the Abakaliki Anticlinorium and adjoining areas (Southeast Nigeria) using magnetic data. Earth Sci. 11:1216198.
Elkhateeb SO, Eldosouky AM. 2016. Detection of porphyry intrusions using analytic signal (AS), Euler Deconvolution, and Centre for Exploration Targeting (CET) Technique Porphyry Analysis at Wadi Allaqi Area, South Eastern Desert, Egypt. Int J Eng Res. 7(6):471–477.
Emeka DN, Usman AH. 2020. Radiometric survey for uranium exploration in the Middle Benue Trough, Nigeria. Nucl Geophys. 34(2):112–120.
Ene EG, Okogbue CO, Dim CIP. 2012. Structural styles and economic potentials of some barite deposits in the Southern Benue Trough, Nigeria. Roman J Earth Sci. 86(1):27–40.
Essa KS, Elhussein M. 2017. A new approach for the interpretation of magnetic data by a 2-D dipping dike. J Appl Geophys. 136:431–443. doi: 10.1016/j.jappgeo.2016.11.022.

Essa KS, Elhussein M. 2018. PSO (particle swarm optimization) for interpretation of magnetic anomalies caused by simple geometrical structures. Pure Appl Geophys. 175(10):3539–3553. doi: 10.1007/s00024-018-1867-0.
Gandhi SS, Prasad N, Charbonneau BW. 1996. Geological and geophysical signatures of a large polymetallic exploration target at Lou Lake, southern great Bear magmatic zone, Northwest Territories. Curr Res. 147–158.
Geological Survey of Canada. 1992. Airborne geophysical survey, Mount Milligan area, British Columbia (NTS 93 O/4W, N/1, N/2E); GSC Open File 2535.
Grasty RL. 1979. Gamma ray spectrometric methods in uranium exploration - theory and operational procedures; in geophysics and geochemistry in the search for metallic ores. Econ Geol Rep Geol Surv Canada 31: 147–161.
Gunn P, Minty B, Milligan P. 1997. The airborne gamma-ray spectrometric response over arid Australian Terranes. In: Gubins A, editor. Proceedings of Exploration 97: Fourth Decennial International Conference on Mineral Exploration. Australia; p. 733–740.
Haruna IV. 2017. Review of the basement geology and mineral belts of Nigeria. J Appl Geol Geophys. 5(1):37–45.
Holden E-J, Dentith M, Kovesi P. 2008. Towards the automatic analysis of regional aeromagnetic data to identify regions prospective for gold deposits. Comput Geosci. 34(11):1505–1513. doi: 10.1016/j.cageo.2007.08.007.
Holden E-J, Kovesi P, Dentith M, Wedge D, Wong JC, Fu SC. 2010. Detection regions of structural complexity within aeromagnetic data using image analysis. Twenty Fifth International Conference of Image and Vision Computing; November 8–9, New Zealand.
Kasidi S, Ndatuwong LG. 2017. Analysis of aeromagnetic data over Middle Benue Trough and its adjourning basement terrain, North Central Nigeria. IOSR J Appl Geol Geophys. 5(5):01–08.
Kovesi K. 1991. Image features from phase congruency. Videre J Comput Vis Res. 1(3).
Kovesi P. 1997. Symmetry and asymmetry from local phase. AI'97, Tenth Australian Joint Conference on Artificial Intelligence; December 1997.
Lam L, Lee S-W, Suen CY. 1992. Thinning methodologies-A comprehensive survey. IEEE Trans Pattern Anal Machine Intell. 14(9):869–885. doi: 10.1109/34.161346.
Lee MK, Peart RJ, Cuss RJ, Jones DG, Beamish D, Vironmaki J. 2001. Application and challenges for high resolution airborne surveys in populated areas. In: EAGE extended abstract. Amsterdam.
Marshall A. 2021. Radiometric methods in mineral exploration. In: Mineral exploration. Springer. p. 113–127.
McClenaghan M. 2017. Airborne magnetic surveys for mineral exploration: principles, practice, and interpretation. Ore Geol Rev. 81:33–49.
Mihalasky M, McClenaghan M, Long D. 2018. Mineral exploration methods. In: Mineral resources in a sustainable world. Springer. p. 31–61.
Milligan P, Gunn P. 1997. Enhancement and presentation of airborne geophysical data. AGSO J. Aust Geol Geophys. 17(2):63–75.
Mineral Resources of the Western US. 2017. The teacher-friendly guide to the Earth scientist of the Western US. http://geology.Teacher friendly guide.Org/index.php/ mineral-w.
Nabighian MN. 1972. The analytical signal of two dimensional magnetic bodies with polygon cross-section: its properties and use for automated anomaly interpretation. Geophysics. 37(3):507–517. doi: 10.1190/1.1440276.
Nabighian MN. 1984. Towards the three-dimensional automatic interpretation of potential field data via generalized Hilbert transforms. Fundamental relations. Geophysics. 49(6):780–786. doi: 10.1190/1.1441706.
Nwankwo C, Ekine A. 2009. Geothermal gradients in the Chad Basin, Nigeria, from bottom hole temperature logs. Int J Phys Sci. 4(12):777–783.
Obaje NG. 2009. Geology and mineral resources of Nigeria. Springer Science & Business Media.
Offler R, Whitford DJ. 1992. Wall-rock alteration and metamorphism of a volcanic-hosted massive sulphide deposit at Que River, Tasmania—petrology and mineralogy. Econ Geol. 87(3):686–705. doi: 10.2113/gsecongeo.87.3.686.
Ofoegbu CO. 1983. Interpretation of aeromagnetic anomalies over the Lower and Middle Benue Trough of Nigeria. Geophys J R Astron Soc. 79(3):813–823. doi: 10.1111/j.1365-246X.1984.tb02870.x.
Ofoegbu CO. 1984a. A model of the tectonic evolution of the Benue Trough of Nigeria. Geol Rundsch. 73(3):1007–1018. doi: 10.1007/BF01820885.
Ofoegbu CO. 1984b. Interpretation of aeromagnetic anomalies over Lower and Middle Benue Trough of Nigeria. Geophys J R Astron Soc. 79(3):813–823. doi: 10.1111/j.1365-246X.1984.tb02870.x.

Ofoegbu CO, Mohan NL. 1990. Interpretation of aeromagnetic anomalies over part of southeastern Nigeria using three-dimensional Hilbert transformation. Pure Appl Geophys. 134(1):13–29. doi: 10.1007/BF00878077.
Ofoegbu CO, Onuoha KM. 1991. Analysis of magnetic data over the Abakaliki Anticlinorium of the Lower Benue Trough, Nigeria. Mar Pet Geol. 8(2):174–183. doi: 10.1016/0264-8172(91)90005-L.
Oha IA, Onuoha KM, Nwegbu AN, Abba AU. 2016. Interpretation of high resolution aeromagnetic data over southern Benue Trough, southeastern Nigeria. J Earth Syst Sci. 125(2):369–385. doi: 10.1007/s12040-016-0666-1.
Okunlola IA, Ojo OJ, Ibrahim M. 2015. Geochemical and petrographic characterization of limestone deposits in the Middle Benue Trough, Nigeria. J Min Geol. 51(2):107–116.
Oladapo MI, Adeoye-Oladapo OO. 2011. Geophysical investigation of barite deposit in Tunga, Northeastern Nigeria. Int J Phys Sci. 6:4760–4774.
Olade MA. 1980. Precambrian metallogeny in West Africa. Geol Rundsch. 69(2):411–428. doi: 10.1007/BF02104546.
Orajaka SO. 1973. Possible metallogenic provinces in Nigeria. Econ Geol. 68(2):278–280. doi: 10.2113/gsecongeo.68.2.278.
Osuji LC, Sule IS, Agbo AF, Obioha A. 2018. Tectonics and sedimentation in the Upper Benue Trough, Nigeria: a review. J Afr Earth Sci. 145:233–243.
Pal SK, Majumdar TJ. 2015. Geological appraisal over the Singhbhum-Orissa Craton, India using GOCE, EIGEN6-C2 and in situ gravity data. Int J Appl Earth Obs Geoinf. 35:96–119. doi: 10.1016/j.jag.2014.06.007.
Paoletti V, Pinto A. 2004. Aeromagnetic and radiometric data filtering at the Vesuvian Volcanic Area. Boll Geofis Teor Appl. 46(2-3):245–259.
Ramadass G, SubhashBabu A, Laxmi GU. 2015. Structural analysis of airborne radiometric data for identification of kimberlites in parts of Eastern Dharwar Craton. Int J Sci Res. 4(4):2375–2380.
Ranjbar H, Hassanzadeh H, Torabi M, Ilaghi O. 2001. Integration and analysis of airborne geophysical data of the Darrehzar area, Kerman Province, Iran, using principal component analysis. J Appl Geophys. 48(1):33–41. doi: 10.1016/S0926-9851(01)00059-3.
Reid A, Allègre C, Minster J. 2019. Magnetic survey of eastern Mediterranean Sea. J Geophys Res. 76(15):3469–3488.
Reijers TJA, Petters SW. 1987. Depositional environments and diagenesis of Albian carbonates on the Calabar Flank, SE Nigeria. J Petrol Geol. 10(3):283–294. doi: 10.1111/j.1747-5457.1987.tb00947.x.
Reyment RA. 1965. Aspects of the geology of Nigeria. Ibadan: Ibadan University. Press; p. 445.
Roest WR, Verhoef J, Pilkington M. 1992. Magnetic interpretation using the 3-D analytic signal. Geophysics. 57(1):116–125. doi: 10.1190/1.1443174.
Salawu NB, Orosun MM, Adebiyi LS, Abdulraheem TY, Dada SS. 2020. Existence of subsurface structures from aeromagnetic data interpretation of the crustal architecture around Ibi, Middle Benue, Nigeria. SN Appl Sci. 2(3):427. doi: 10.1007/s42452-020-2230-5.
Schroeter TG. 1995. Porphyry deposits of the northwestern cordillera of North America. Can Inst Min Metall Petrol. 46:888.
Shives RBK, Charbonneau BW, Ford KL. 1997. The detection of potassic alteration by gamma-ray spectrometry—recognition of alteration related to mineralization. In: Proceedings of Exploration 97: Fourth Decennial International Conference on Mineral Exploration. p. 741–752.
Shives RBK, Ford KL, Charbonneau BW. 1995. Applications of gamma ray spectrometric/magnetic/VLF-EM surveys—Workshop Manual; Geological Survey of Canada. Open File. 3061:82.
Smith RS, Thurston JB, Dai T, MacLeod IN. 1998. iSPITM the improved source parameter imaging method1. Geophys Prospect. 46(2):141–151. doi: 10.1046/j.1365-2478.1998.00084.x.
Talwani M, Hiertzler JR. 1964. Computation of magnetic anomalies caused by two dimensional bodes of arbitrary shape. Geol Sci. 9:464–480.
Talwani M, Worzel JL, Landisman M. 1959. Rapid gravity computations for 2 dimensional bodies with application to the Mendocino submarine fracture zone. J Geophys Res. 64(1):49–59. doi: 10.1029/JZ064i001p00049.
Telford W, Gelbert I, Sheritt R. 1990. Applied geophysics. 2nd ed. London: Cambridge University Press.
Thurston JB, Smith RS. 1997. Automatic conversion of magnetic data to depth, dip, and susceptibility contrast using SPITM method. Geophysics. 62(3):807–813. doi: 10.1190/1.1444190.
Thurston JB, Smith RS, Guillon JC. 2000. A multi-model method for depth estimation from magnetic data. Geophysics. 67(2):555–561. doi: 10.1190/1.1468616.
Ugwu G, Ugwu S, Akaegbobi I. 2015. Exploration potential and industrial application of selected Nigerian kaolins. J Afr Earth Sci. 111:173–182.

Uma KO. 1998. The brine fields of the Benue Trough, Nigeria: a comparative study of geomorphic, tectonic and hydrochemical properties. J Afr Earth Sci. 26(2):261–275. doi: 10.1016/S0899-5362(98)00009-8.

Wemegah DD, Preko K, Noye RM, Boadi B, Menyeh A, Danuor SK, Amenyoh T. 2015. Geophysical Interpretation of possible gold mineralization zones in Kyerano, South-Western Ghana using aeromagnetic and radiometric datasets. GEP. 03(04):67–82. doi: 10.4236/gep.2015.34008.

Wilford J, Bierwirth P, Craig M. 1997. Application of airborne gamma-ray spectrometry in soil or regolith mapping and applied geomorphology. J Aust Geol Geophys. 17(2):201–216.

Woakes M, Rahaman MA, Ajibade AC. 1987. Some metallogenetic features of the Nigerian Basement. J Afr Earth Sci. 6(5):655–664. doi: 10.1016/0899-5362(87)90004-2.

Won IJ, Bevis M. 1987. Computing the gravitational and magnetic anomalies due to a polygon: algorithms and Fortran subroutines. Geophysics. 52(2):232–238. doi: 10.1190/1.1442298.